A NUMERICAL HEAT TRANSFER STUDY OF PROFILE CALIBRATION

J. M. Nóbrega[(1)], O. S. Carneiro[(1)], J. A. Covas[(1)], P. J. Oliveira[(2)], F. T. Pinho[(3)]

[(1)] IPC - Institute of Polymer and Composites, Department of Polymer Engineering, University of Minho, Campus de Azurém, 4800-058 Guimarães, Portugal

[(2)] Departamento de Engenharia Electromecânica, Universidade da Beira Interior, Rua Marquês D'Ávila e Bolama, 6200 Covilhã, Portugal

[(3)] CEFT - Centro de Estudos de Fenómenos de Transporte, Departamento de Engenharia Mecânica, Universidade do Minho, Campus de Azurém, 4800-058 Guimarães, Portugal

Abstract

A 3D numerical code, based on the finite volume method, developed to model the cooling stage along an extrusion line is presented and validated prior to being used for investigating the effect of various process and geometrical parameters onto the efficiency of calibration/cooling units. The code is able to tackle accurately various practical situations such as the presence of several individual cooling units and the existence of a thermal resistance between the plastic profile and the cooling medium.

The code was validated through the comparison of the numerical predictions with the analytical solution of a simple problem and with results produced by a commercial software.

The detailed investigation of the calibration unit has shown that most of the heat is removed at the calibrator via the cooling channels and that the contact resistance at the interface is the most important parameter affecting the performance of the unit. Additionally, it was shown that boundary conditions on the calibrator/extrudate outer surfaces have negligible impact.

The effect of process and geometrical parameters on the cooling performance can be quite distinct. Often, when a higher reduction of the profile average temperature is imparted, lower temperature homogeneity is also obtained, which is undesirable; exceptions are variations in the extrusion velocity and splitting the calibrator into several units.

Introduction

A typical plastics extrusion line for the production of profiles comprises an extruder, a die, a calibration/cooling table (which can include several units), a haul-off and a saw (or, alternatively, a coiling device). The viscoelastic nature of the polymer melt, together with unavoidable fluctuations of the operating conditions (which affect the rheological behaviour and flow dynamics), make it very difficult to produce an extrudate with the required cross-section. Moreover, as the profile progresses along the production line, it is subjected to a variety of external forces (such as friction, gravity, buoyancy and compression), which can cause important deformations, unless efficient cooling assures enough profile strength [1, 2]. Therefore, the calibration/cooling step has a double objective: it determines the final dimensions of the profile, while cooling it down fast to solidify the outer layers of the extrudate to ensure sufficient rigidity during the remainder cooling steps [1]. Cooling of the extrudate should be as uniform as possible, meaning that the temperature gradients along the profile contour and thickness should be minimized, in order to induce the adequate morphology development and a reduced level of residual thermal stresses [3, 4].

Despite their obvious practical relevance, calibrating and cooling systems have attracted relatively little attention in the scientific literature. Most available reports concern the calculation of the time evolution of the extrudate temperature [5-7], the exception being the work of Fradette *et al.* [3], in which the model previously developed [6] was integrated in an optimisation routine used to determine the optimal location and size of the cooling channels. However, a thorough study of the influence of the above geometrical, material, process and operational parameters on the cooling performance is apparently not available. In fact, the existing results are either qualitative or concentrate on a few variables [7, 8] ignoring, for instance, the effect of boundary conditions. Moreover, no methodology for the design of calibrators has yet been proposed.

This work presents and validates a 3D code based on the finite-volume method (FVM) to model the thermal interchanges during the calibration and cooling stage of profile extrusion. FVM software is faster and requires less computational resources than its FEM counterpart [9], which is essential for the recurring use required by the optimization algorithm. With a view to design, a study of the influence of the boundary conditions, geometrical and operating parameters on the performance of cooling is also carried out.

Outline of the numerical procedure

The thermal field in the calibrating and cooling system is calculated by a 3D computational code based on the finite-volume method. The code is used to numerically calculate the variation of the temperature field within the extrudate as well as within the calibrator. Therefore, the energy conservation equations to be solved here can be written as

$$\frac{\partial}{\partial x}\left(k_p \frac{\partial T_p}{\partial x}\right)+\frac{\partial}{\partial y}\left(k_p \frac{\partial T_p}{\partial y}\right)+\frac{\partial}{\partial z}\left(k_p \frac{\partial T_p}{\partial z}\right)-\frac{\partial}{\partial z}\left(\rho_p c_p w T_p\right)=0 \qquad (1)$$

for the profile, and as

$$\frac{\partial}{\partial x}\left(k_c \frac{\partial Tc}{\partial x}\right)+\frac{\partial}{\partial y}\left(k_c \frac{\partial T_c}{\partial y}\right)+\frac{\partial}{\partial z}\left(k_c \frac{\partial Tc}{\partial z}\right)=0 \qquad (2)$$

for the calibrator, where T is the medium temperature, w is the longitudinal velocity component (extrusion direction) in a Cartesian co-ordinate frame, ρ is the fluid density, k is the thermal conductivity and c is the specific heat. The subscripts p and c denote polymer and calibrator, respectively.

In order to take into account real processing conditions, various temperature and heat flux boundary conditions were implemented. At the interface between the profile and the calibrator, either perfect contact, assuming both temperature and heat flux continuity,

$$\left(T_p = T_c\right)_{\text{interface}} \qquad (3)$$

$$k_c\left(\frac{\partial T_c}{\partial n}\right)_{\text{interface}} = -k_p\left(\frac{\partial T_p}{\partial n}\right)_{\text{interface}} \qquad (4)$$

or the existence of a temperature discontinuity (i.e., a thermal contact resistance [10])

$$k_c\left(\frac{\partial T_c}{\partial n}\right)_{\text{interface}} = -k_p\left(\frac{\partial T_p}{\partial n}\right)_{\text{interface}} = h_i\left(T_p - T_c\right)_{\text{interface}} \quad (5)$$

were considered. Here, h_i is the interface heat transfer coefficient. At the interface between the outside walls of the calibrator and the surrounding air, or between the external extrudate surface and the surrounding air, adiabatic or natural convection and radiation boundary conditions were set up. Figure 1 summarizes the boundary conditions considered in a typical problem.

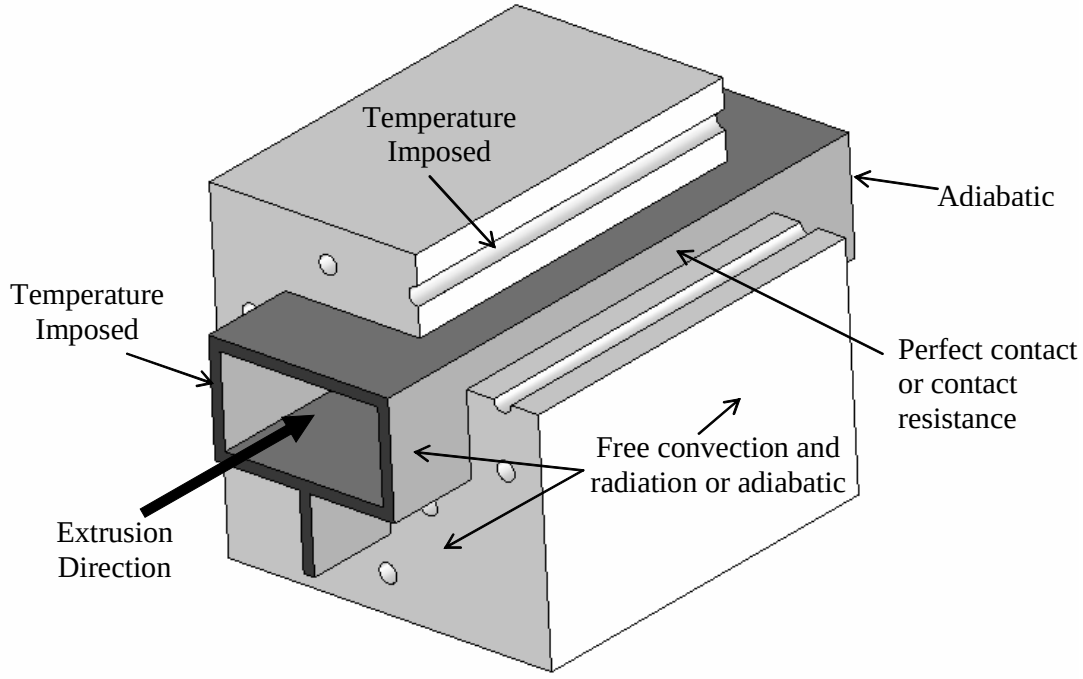

Figure 1 - Thermal boundary conditions considered.

Equations (1) and (2) are discretised following a finite-volume approach and the resulting sets of linear algebraic equations are solved iteratively and sequentially, assuming an imposed heat flux at the polymer/calibrator interface. The coupling between the temperature fields in the polymer and calibrator domains is dealt with as follows. At each iteration step, the interface temperatures obtained for both domains are used to update the interface heat flux values (which depend on the type of boundary condition assumed at the interface), by using either Equation (4) or (5), and the whole procedure is repeated until the temperature field converges.

Model Assessment

Direct confrontation between predictions and experimental data is difficult, since the practical measurement of the temperature profiles within and along the extrudate cross-section progressing along the calibration/cooling system, is extremely difficult, requiring the use of thermocouples imbedded in the material at different depths of the profile thickness, and moving with the profile [5]. Profile surface temperatures between two consecutive calibrators are easier to monitor, but the quality of the measurements depends on the emissivity settings used in the non-contact infrared thermometers that are generally employed and also on the measuring depth,

i.e., the thickness effectively reached by the radiation from the sensor [11]. However, most of the temperature measurements reported concern pipes [1, 5, 12-14] rather than profiles [10] and, even in this case, the data presented are insufficient for modelling purposes. Therefore, the model developed and presented in this work was assessed by confronting its predictions with: i) analytical results derived for a simple geometry and ii) calculations provided by a general purpose FEM software [15].

Analytical solution

The first case study considered is illustrated in Figure 2. It consists of two rectangular slabs, S1 and S2, with thermal conductivities k_1 and k_2, respectively, under contact through one of their faces. As shown also in the figure, the temperature is imposed on the remaining faces.

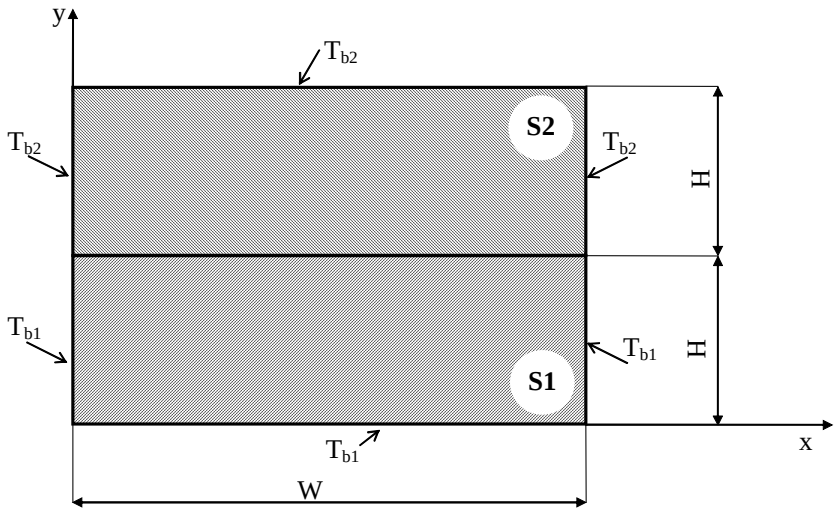

Figure 2 - Geometry and boundary conditions for the 'Analytical' problem.

As shown in [16] the temperature distribution in each slab can be obtained from:

$$T = T_{b1} + \sum_{n=1}^{\infty} \frac{2}{\pi}\left(T_{b2} - T_{b1}\right)\frac{(-1)^{n+1}+1}{n}\frac{-k_2}{\left(k_2+k_1\right)}\sin\left(\frac{n\pi x}{W}\right)\sinh\left(\frac{n\pi y}{W}\right) \qquad (6)$$

for S1, and:

$$T = T_{b2} + \sum_{n=1}^{\infty} \frac{2}{\pi}\left(T_{b2} - T_{b1}\right)\frac{(-1)^{n+1}+1}{n}\frac{k_1}{\left(k_2+k_1\right)}\sin\left(\frac{n\pi x}{W}\right)\sinh\left(\frac{n\pi(-y+2H)}{W}\right) \qquad (7)$$

for S2, for the perfect contact case, and by:

$$T = T_{b1} + \sum_{n=1}^{\infty} \left[\frac{2}{\pi} h_i (T_{b1} - T_{b2}) \frac{(-1)^{n+1} + 1}{n} \right.$$

$$\left. \frac{1}{-k_1 \frac{n\pi}{W} \cosh\left(\frac{n\pi H}{W}\right) - \left(\frac{k_2 + k_1}{k_2}\right) \sinh\left(\frac{n\pi H}{W}\right)} \sin\left(\frac{n\pi x}{W}\right) \sinh\left(\frac{n\pi y}{W}\right) \right] \tag{8}$$

for S1 and from:

$$T = T_{b1} + \sum_{n=1}^{\infty} \left[\frac{2}{\pi} h_i (T_{b1} - T_{b2}) \frac{(-1)^{n+1} + 1}{n} \right.$$

$$\left. \frac{1}{k_2 \frac{n\pi}{W} \cosh\left(\frac{n\pi H}{W}\right) + \left(\frac{k_2 + k_1}{k_1}\right) \sinh\left(\frac{n\pi H}{W}\right)} \sin\left(\frac{n\pi x}{W}\right) \sinh\left(\frac{n\pi(-y + 2H)}{W}\right) \right] \tag{9}$$

for S2, when the interface is modelled with a contact resistance boundary condition.

The temperature distributions defined by Equations (6-9) for perfect contact and thermal resistance, are compared in Figure 3 with those obtained in the numerical code, using W=100 mm, H=50 mm, T_{b1}=100 ºC, T_{b2}=180 ºC, k_1=7 W/mK, k_2=14 W/mK and, for the case of contact resistance, h_i=500 W/m^{2}K. It is clear that the two sets of results are virtually coincident hence giving confidence on the correct implementation of the thermal routines.

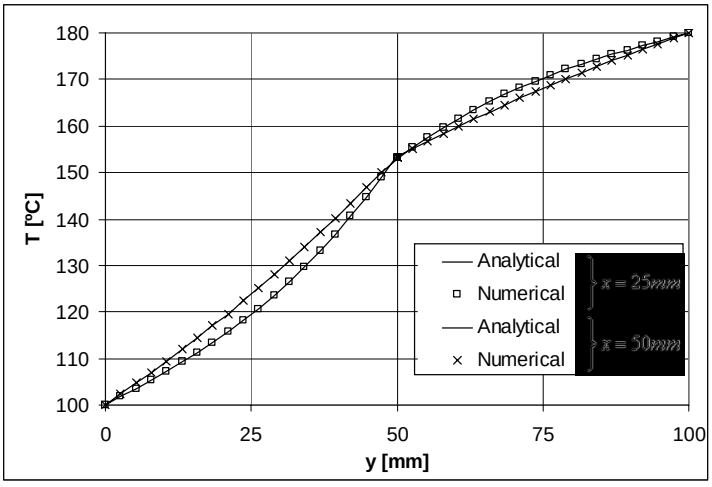

(a)

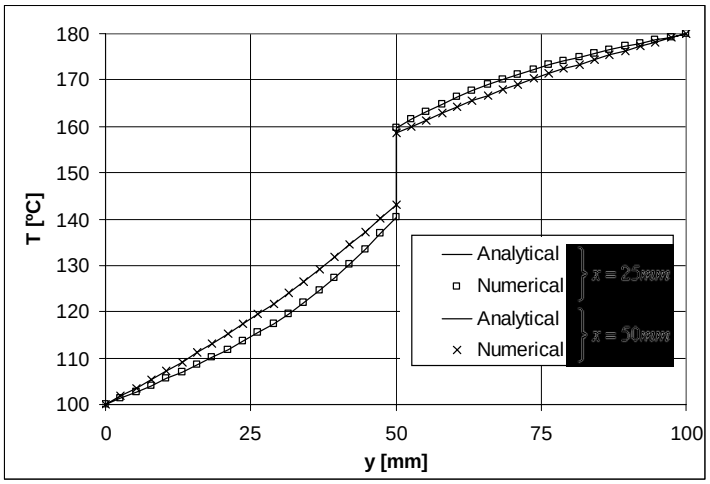

(b)

Figure 3 - Analytical and numerical results for the temperature distribution of the 'Analytical' problem: (a) perfect contact; (b) contact resistance.

Complex layout

The predictions of the numerical routines developed were also compared with the results obtained by a commercial software Polyflow [15] for the problem shown in Figure 4. The problem consists of the determination of the temperature distribution in a 2 mm thick polymeric sheet moving at 0.01 m/s while being cooled by a 50 mm long and 10 mm thick calibrator containing three transverse cooling channels. The thermal and physical properties of the calibrator (subscript c) and polymer (subscript p) are: k_p=0.18 W/mK, k_c=23.0 W/mK, ρ_p=1400 kg/m^3 and c_p=1000 J/kgK. The thermal boundary conditions are also identified in Figure 4.

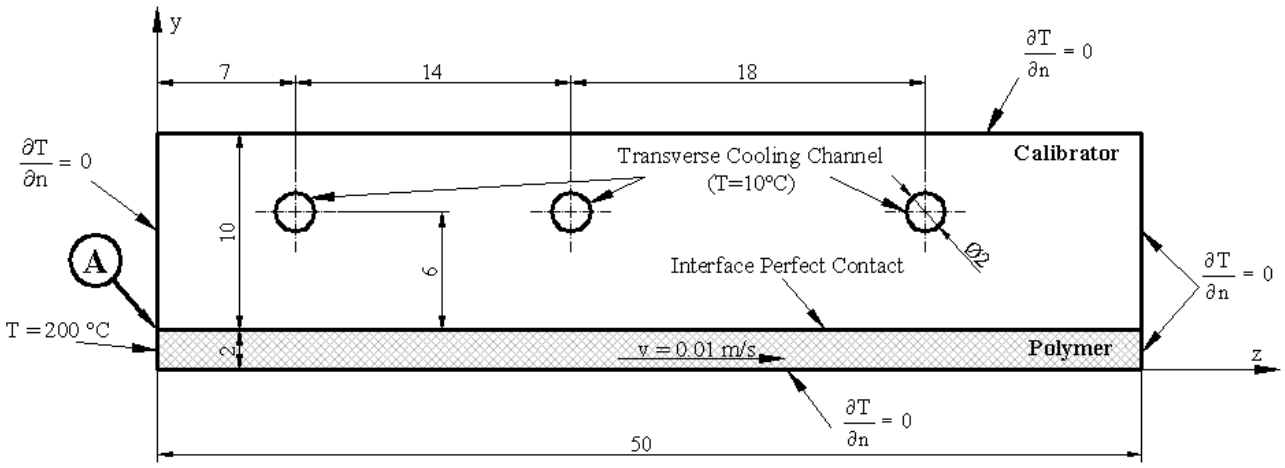

Figure 4 - Description of the 'Complex Layout' problem.

The agreement observed between both solutions can be confirmed in Figure 5 that compares temperature profiles across the sheet at three different axial locations (z/L= 7/50, 30/50 and 50/50, where L is the length of the calibrator).

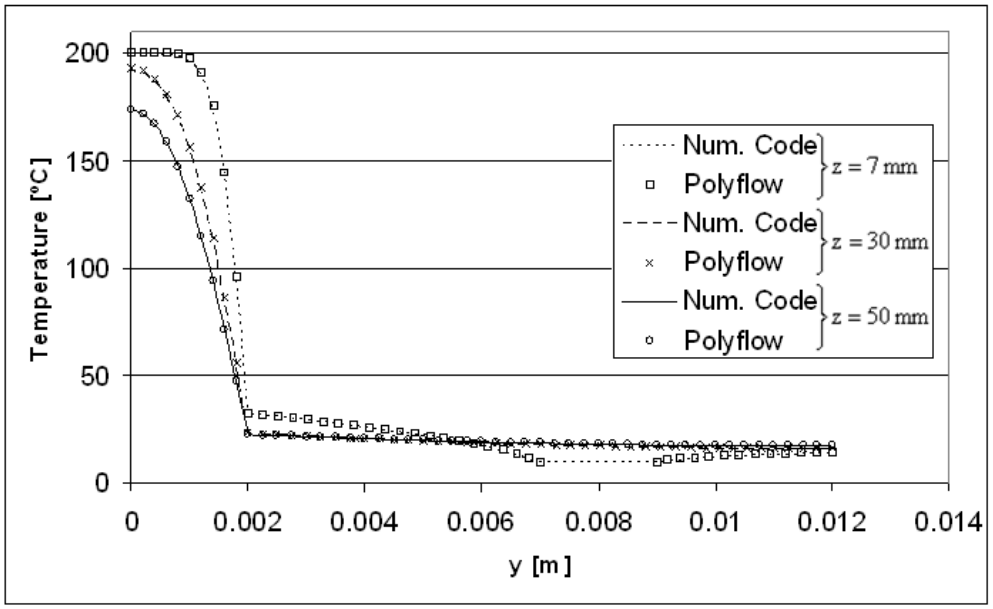

Figure 5 - Temperature distributions for the 'Complex Layout' problem of Figure 4 (z/L = 7/50; z/L = 30/50; z/L = 50/50).

Influence of Boundary Conditions, Process and Geometrical Parameters

Next, the code was used to investigate the effect of some boundary conditions, process and geometrical parameters on the behaviour and performance of calibrating/cooling systems. For this purpose the cooling of the rectangular hollow profile shown in Figure 6 was studied under the general conditions summarized in Table 1. A calibration length of 600 mm was fixed but it corresponded to either a single or three consecutive calibration units. The results obtained with the various systems were compared in terms of heat fluxes at the geometry boundaries and of minimum (T_{min}), maximum (T_{max}) and average ($\overline{T}$) temperatures and the temperature distribution standard deviation (σ_T) calculated at the end cross section of the polymer extrudate, which is a measure of the temperature non-homogeneity at the final cross section, i.e., at the end of the problem domain.

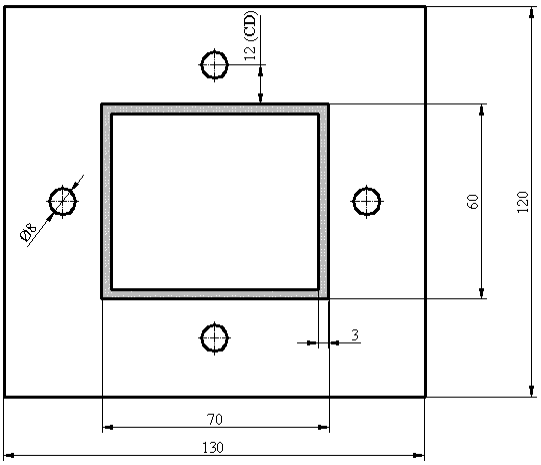

(a)

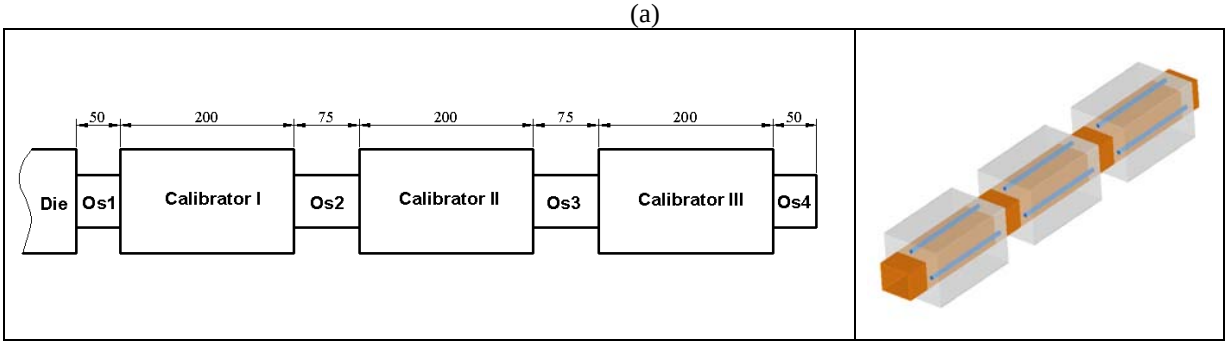

(b)

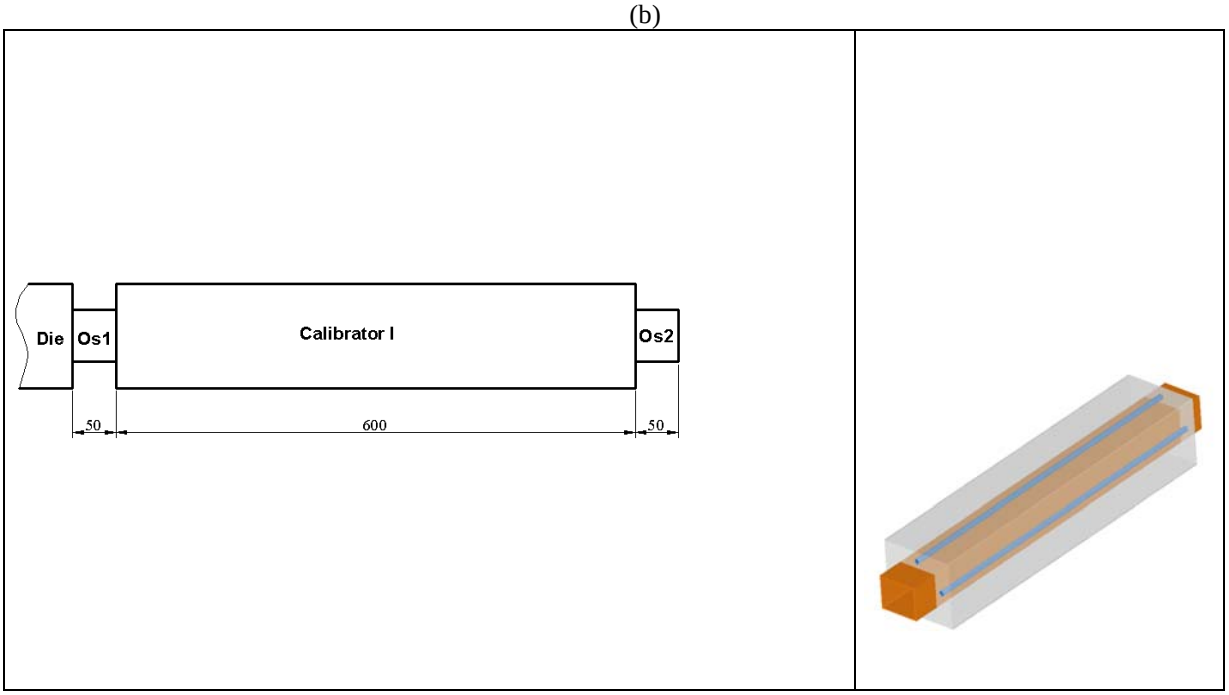

(c)

Figure 6 - Cooling of a rectangular hollow profile problem: cross section geometry (a), three calibrators layout (b) and one calibrator layout (c).

Table 1 – General conditions used in the simulations.

k_p	0.18 W/mK
k_c	14.0 W/mK
□$_p$	1400 kg/m^3
c_p	1000 J/kgK
Linear extrusion velocity	2 m/min
Profile thickness	3 mm
Cooling channels' diameter	8 mm
Melt inlet temperature	180 ºC
Room temperature	20 ºC
Cooling fluid temperature	18 ºC
Profile/air convection heat transfer coefficient (free convection)	5 W/m^{2}K
Polymer emissivity ε_p	0.9
Calibrator emissivity ε_c	0.25
Profile/calibrator convection heat transfer coefficient (contact resistance)	500 W/m^{2}K
Inner profile boundary	Insulated
CD	12 mm

It is worth mentioning that the results obtained for the profile geometry under study cannot be directly extrapolated to other geometries but, nevertheless, provide information onto the qualitative effect of the main variables involved in the process and their relative importance.

Boundary conditions

An important issue for modelling the profile cooling stage is the definition of the boundary conditions at the profile and calibrator surfaces. In the literature, the outer surfaces of both profile and calibrator are modelled either as adiabatic [6] or having a defined convective heat flux [5], always neglecting radiation. For the interface between the profile and the calibrator either perfect contact or contact resistance is used, with some authors arguing that the contact resistance is the best choice [1], but without any practical or computational quantification of its relevance. Thus, in order to study the influence of this parameter, cooling of the profile presented in Figure 6(a) was modelled adopting the layout shown in Figure 6(b), where the cooling length of 600 mm was divided into three 200 mm long calibrators, separated by 75 mm long annealing zones. In this Figure, Os1 to Os4 represents the profile outer surfaces, i.e., those exposed to the surrounding environment along the cooling line. The set of case studies considered is described in Table 2, while the computed results are summarized in Tables 3 and 4.

Table 2 – Case studies considered to study the influence of the boundary conditions.

Code	Boundary for outer surface of profile+calibrator	Calibrator/Profile Interface [W/m^{2}K]
c1r1	convection+radiation	h_i=500
c0r0	adiabatic	h_i =500
c1r0	convection	h_i =500
c0r1	radiation	h_i =500
h↑ (+50%)	convection+radiation	h_i =750
h↓ (-50%)	convection+radiation	h_i =250
pc	convection+radiation	Perfect contact

Table 3 – Boundary heat fluxes [W] computed for the case studies listed in Table 2.

Code	Os1	Calibrator I		Os2	Calibrator II		Os3	Calibrator III		Os4	Total
		Calibrator surface	Cooling channels		Calibrator surface	Cooling channels		Calibrator surface	Cooling channels		
c1r1	-32.0	-1076.1		-20.7	-736.3		-15.0	-589.8		-7.5	-2477.3
		-15.9	-1060.2		-10.2	-726.1		-7.8	-581.9		
c0r0	0.0	-1089.0		0.0	-748.8		0.0	-601.1		0.0	-2438.9
		0.0	-1089.0		0.0	-748.8		0.0	-601.1		
c1r0	-10.3	-1085.9		-8.3	-744.4		-6.3	-596.7		-3.3	-2455.3
		-12.3	-1073.6		-8.0	-736.4		-6.2	-590.6		
c0r1	-22.3	-1079.0		-12.9	-740.5		-9.0	-593.9		-4.3	-2461.8
		-4.0	-1075.0		-2.5	-738.0		-1.9	-592.0		
h↑	-32.0	-1172.7		-18.9	-773.0		-13.5	-609.3		-6.5	-2626.0
		-17.5	-1155.2		-10.8	-762.1		-8.1	-601.1		
h↓	-32.0	-859.9		-24.9	-638.0		-19.0	-530.9		-9.9	-2114.4
		-12.3	-847.5		-8.6	-629.3		-6.9	-524.0		
pc	-32.1	-1421.7		-14.9	-848.0		-10.1	-643.8		-4.6	-2975.2
		-21.9	-1399.8		-12.1	-835.9		-8.8	-635.0		

Table 3 compares the heat fluxes at the various boundaries. Starting with the reference case study *c1r1*, which accounts both convection and radiation at the outer boundaries, the table shows losses of 32.0, 20.7, 15.0 and 7.5 W through the extrudate outer surfaces Os1 through Os4, respectively, and losses of 1076.1, 736.3 and 589.8 in the three calibrators mostly via the cooling channels. Table 4 contains data for temperature at the final cross section. As shown in Table 3, most of the heat is removed from the profile through its interface with the calibrator, and then from the calibrator through the cooling channels. Consequently, the values in Table 4 are little affected by the type of boundary condition considered at the extrudate and calibrator outer

surfaces, and, in contrast, the conditions at the interface between the extrudate and the calibrator are fundamental as can be seen in the total loss. In fact, changes in the resistance coefficient (h_i) have the highest impact on the total heat loss (compare h↑, h↓ and pc with the reference case). The effects of radiation and convective heat transfer are similar but since most of the cooling takes place via the cooling channels the type of outer boundary has a negligible impact upon the total loss. However, the usual procedure of considering only convection is inadequate. Anyway, if detailed knowledge of temperature along the extrudate is required, then it is important to consider both the effects of convection and radiation in the annealing zones.

Table 4 – Results computed at the end cross section of the extrudate for the case studies of Table 2 (V- Value, D- Relative difference to reference problem *c1r1*).

Code		T_{min}	T_{max}	$\overline{T}$	σ_T
c1r1	V	48.9	136.1	107.9	21.0
	D	--	--	--	--
c0r0	V	51.2	137.0	109.0	20.8
	D	4.7%	0.7%	1.0%	-1.3%
c1r0	V	50.1	136.6	108.6	20.9
	D	2.4%	0.4%	0.6%	-0.6%
c0r1	V	50.0	136.5	108.4	20.9
	D	2.2%	0.3%	0.4%	-0.6%
h↑ (+50%)	V	57.9	143.3	118.5	19.1
	D	-6.1%	-2.3%	-4.0%	3.2%
h↓ (-50%)	V	45.9	133.0	103.6	21.7
	D	18.4%	5.3%	9.8%	-9.3%
pc	V	40.2	125.4	93.4	22.9
	D	-17.9%	-7.8%	-13.4%	8.9%

Finally, it is worth noting that a 50% change of h_i, which lies within the practical range of variation, yields a lower than 10% change in $\overline{T}$ of the extrudate at the end of the cooling zone, in agreement with the variations in the total heat loss. Clearly this parameter is the major factor affecting the thermal performance of the production line.

Process and geometrical parameters

To assess the influence of process and geometrical parameters on cooling, the conditions specified in Table 1 and the layout shown in Figure 6(c) (i.e., single 600 mm long calibrator) was considered. Table 5 presents a number of case studies used to investigate the effect of changes in the conditions defined in Table 1, which will be taken as the reference case (*ref*). Figure 7 illustrates the changes in the layout of the cooling channels, and the corresponding results are listed in Table 6.

Table 5 – Case studies considered to study the influence of process and geometrical parameters.

	Code	Parameter	Description
Process Parameters	*tw*↓	Cooling fluid temperature	T_w = 12ºC
	tw↑		T_w = 24ºC
	vp↓	Profile velocity	v_p = 1 m/min
	vp↑		v_p = 3 m/min
Geometrical Parameters	*nc*	Number of Calibrators	The total cooling length is divided by three individual calibrators (Figure 6(b)).
	la	Cooling channel layout	Four cooling channels close to the profile's corner (Figure 7(a))
	lb		Two cooling channels next to each profile side (Figure 7(b))
	lc		Top and bottom cooling channels in a narrow zig-zag arrangement (Figure 7(c))
	ld		Top and bottom cooling channels in a wide zig-zag arrangement (Figure 7(d))
	cd↓	Distance of cooling channel to profile surface (CD in Figure 6(a))	CD = 8 mm
	cd↑		CD = 16 mm
	dw↓	Cooling channel diameter	d = 4 mm
	dw↑		d = 12 mm

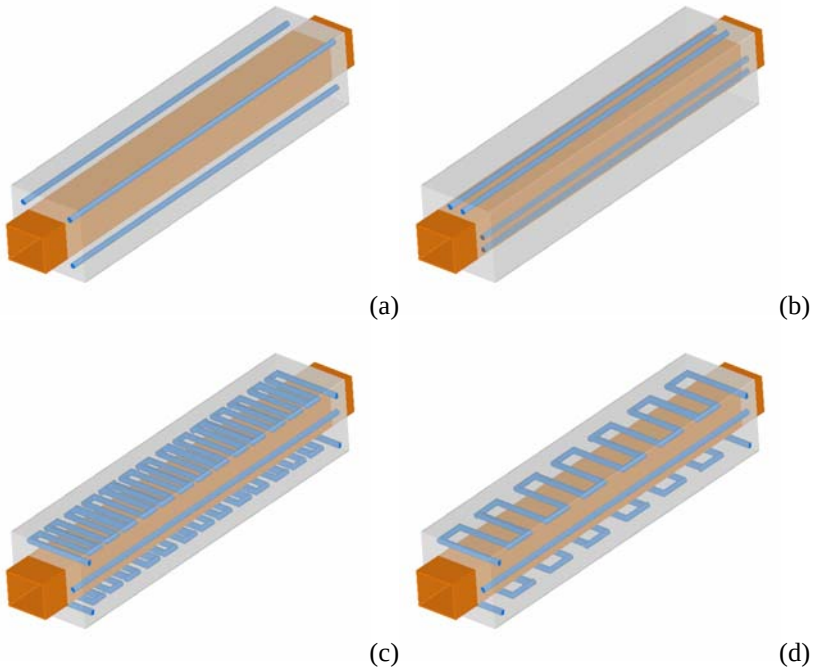

Figure 7 - Variations of the layout of the cooling system (see Table 5): cooling channels close to the profile's corners '*la*' (a), two cooling channels close to each profile side '*lb*' (b), narrow pitch zig-zag arrangement '*lc*' (c) and wide pitch zig-zag arrangement '*ld*' (d).

Table 6 – Results computed at the end cross section of the extrudate and total heat lost for the case studies of Table 5. (V- Value, D- relative difference to reference problem).

	Code		T_{min} [ºC]	T_{max} [ºC]	$\overline{T}$ [ºC]	σ_T [ºC]	Total heat removed [W]
	ref	V	48.7	142.9	111.9	23.3	2340.5
Process Parameters	*tw*↓	V	44.3	141.6	109.5	24.1	2424.6
		D	-9.1%	-0.9%	-2.2%	3.5%	3.6%
	tw↑	V	53.1	144.2	114.4	22.5	2256.4
		D	9.1%	0.9%	2.2%	-3.5%	-3.6%
	vp↓	V	38.9	99.0	79.1	13.4	1787.0
		D	-20.1%	-30.7%	-29.3%	-42.4%	-23.6%
	vp↑	V	55.3	161.9	128.2	27.2	2697.8
		D	13.4%	13.3%	14.6%	16.9%	15.3%
Geometrical Parameters	*nc*	V	48.9	136.1	107.9	21.0	2477.3
		D	0.4%	-4.8%	-3.6%	-9.6%	5.8%
	la	V	44.4	146.7	116.0	23.0	2200.9
		D	-8.8%	2.6%	3.6%	-1.3%	-6.0%
	lb	V	41.4	139.3	107.9	24.2	2478.9
		D	-15.1%	-2.5%	-3.6%	3.9%	5.9%
	lc	V	32.4	137.4	104.2	25.5	2606.8
		D	-33.6%	-3.8%	-6.9%	9.5%	11.4%
	ld	V	33.6	137.7	105.3	25.3	2567.6
		D	-31.1%	-3.6%	-5.9%	8.6%	9.7%
	cd↓	V	48.7	142.8	110.9	23.5	2373.6
		D	-0.1%	-0.1%	-0.9%	0.9%	1.4%
	cd↑	V	50.1	143.5	113.5	22.9	2286.3
		D	2.8%	0.4%	1.4%	-1.5%	-2.3%
	dw↓	V	52.3	144.4	114.2	22.7	2261.0
		D	7.3%	1.0%	2.1%	-2.3%	-3.4%
	dw↑	V	46.1	141.6	110.0	23.7	2407.5
		D	-5.5%	-0.9%	-1.7%	1.8%	2.9%

The effect of the cooling fluid temperature (*tw*) is much smaller than that of the profile velocity (*vp*). Additionally, the effect of *tw* with respect to $\overline{T}$ and σ_T is conflicting, i.e., values that promote a lower $\overline{T}$ will induce higher σ_T and vice-versa, as a consequence of the high Biot number that characterises heat transfer in plastics. Conversely, *vp* promotes the simultaneous increase or decrease of both $\overline{T}$ and σ_T, which is advantageous for optimisation purposes. However, a better cooling performance (which requires low values of $\overline{T}$ and σ_T) involves, not surprisingly, the decrease of *vp*, i.e., of the production rate.

In the case of geometrical parameters, the use of a zig-zag arrangement for the cooling channels (*lc*,*ld*), or the increase of the number of cooling channels (*lb*), favours the decline of T_{min}, T_{max} and $\overline{T}$, but again increase σ_T. The improvements obtained by narrowing a zig-zag arrangement (*lc*) are negligible compared with the use of a wider one (*ld*). In practice, these marginal advantages will eventually be offset by the higher machining costs.

The distance between the cooling channels and the profile surface (*cd*) is relatively unimportant; its reduction (*cd*↓**)** has almost no effect on the results, while its increase (*cd*↑**)** reduces the cooling efficiency. This indicates a limiting *cd* value below which the increase in cooling efficiency in negligible.

Splitting the calibrator into several smaller units with the same total length (*nc*) promoted variations of $\overline{T}$ and σ_T with the same sign and is advantageous in relation to the reference case. This is a consequence of the reduction of the heat flux at the polymer surface occurring in-between two consecutive calibrators, which increases both the temperature homogeneity and the effectiveness of the subsequent cooling, given the increase of the profile surface temperature. Therefore, splitting the calibrator has a thermal effect similar to that of reducing the extrusion velocity (*vp*↓), but without affecting the production rate. In terms of the values obtained for $\overline{T}$ and 'total heat removed', it can be concluded that this option has a performance similar to that of layout *lb*, which employs a double number of cooling channels.

Finally, having the cooling channels close to the profile corners (*la*) reduces T_{min} but increases T_{max}, because the profile corners cool more efficiently than the center.

Conclusions

A 3D FVM code developed to model the cooling stage of an extrusion line was presented and validated prior to being used for investigating the effect of various process and geometrical parameters onto the efficiency of calibration/cooling units. The code is able to tackle accurately various practical situations such as the presence of several individual cooling units and the existence of a thermal resistance between the plastic profile and the cooling medium.

The detailed investigation of the calibration unit has shown that most of the heat is removed at the calibrator via the cooling channels and that the contact resistance at the interface is the most important parameter affecting the performance of the unit. Additionally, it was shown that boundary conditions on the calibrator/extrudate outer surfaces have negligible impact.

The effect of process and geometrical parameters on the cooling performance can be quite distinct. Often, when a reduction of the profile average temperature is imparted, lower temperature homogeneity is also obtained, but exceptions are variations in the extrusion velocity and splitting the calibrator into several units. Since the extrudates are characterised by high Biot numbers, significant increases in the heat transfer removal at the extrudate surface quickly reach a limiting behaviour (in terms of efficiency) and this should be taken into consideration when designing calibration/cooling units.

References

[1] - V. Kleindienst, Kunststoffe. **63**(1), 7-11 (1973).

[2] - W. Michaeli, *Extrusion Dies for Plastics and Rubber: Design and Engineering Computations*. 2nd ed. Spe Books, Munich, Vienna, New York: Hanser Publishers. (1992)

[3] - L. Fradette, P. A. Tanguy, F. Thibault, P. Sheehy, D. Blouin, and P. Hurez, Journal of Polymer Engineering. **14**(4), 295-322 (1995).
[4] - R. J. Brown. Predicting How the Cooling and Resulting Shrinkage of Plastics Affect the Shape and Straightness of Extruded Profiles. in *Antec 2000*. Orlando, Florida, U.S.A. (2000)
[5] - J. F. T. Pittman, G. P. Whitham, S. Beech, and D. Gwynn, International Polymer Processing. **9**(2), 130-140 (1994).
[6] - P. Sheehy, P. A. Tanguy, and D. Blouin, Polymer Engineering and Science. **34**(8), 650-656 (1994).
[7] - L. Placek, J. Svabik, and J. Vlcek. Cooling of Extruded Plastic Profiles. in *Antec 2000*. Orlando, Florida, U.S.A. (2000)
[8] - I. Szarvasy and R. Sander, Kunststoffe-Plast Europe. **89**(6), 7-9 (1999).
[9] - J. Vlachopoulos. Recent Progress and Future Challenges in Computer-Aided Polymer Processing Analysis and Design. in *ATV-Semapp Meeting*. Funen, Odense, Denmark (1998)
[10] - L. Fradette, P. A. Tanguy, P. Hurez, and D. Blouin, International Journal of Numerical Methods for Heat & Fluid Flow. **6**(1), 3-12 (1996).
[11] - W. Obendrauf, G. R. Langecker, and W. Friesenbichler, International Polymer Processing. **13**(1), 71-77 (1998).
[12] - J. F. T. Pittman, I. A. Farah, D. H. Isaac, and A. Eccott. Transfer Coefficients in Spray Cooling of Plastic Pipes. in *Plastics Pipes IX*. Edinburgh, U. K. (1995)
[13] - J. F. T. Pittman and I. A. Farah, Plastics, Rubber and Composites Processing and Applications. **25**(6), 305-12 (1996).
[14] - J. F. T. Pittman, G. P. Whitham, and I. A. Farah, Polymer Engineering and Science. **35**(11), 921-928 (1995).
[15] - Polyflow, Fluent Inc. (http://www.fluent.com).
[16] - J. M. Nóbrega, *Computer Aided Design of Forming Tools for the Production of Thermoplastic Profiles*, PhD Thesis, University of Minho: Guimarães, Portugal.